Macromolecules

pubs.acs.org/Macromolecules Article

Efficient Synthesis of Asymmetric Miktoarm Star Polymers

Adam E. Levi, Liangbing Fu, Joshua Lequieu, Jacob D. Horne, Jacob Blankenship, Sanjoy Mukherjee, Tianqi Zhang, Glenn H. Fredrickson, Will R. Gutekunst, and Christopher M. Bates*

Cite This: *Macromolecules* 2020, 53, 702−710 Read Online

ACCESS | Metrics & More | Article Recommendations | Supporting Information

ABSTRACT: Asymmetric miktoarm star polymers produce unique material properties, yet existing synthetic strategies are beleaguered by complicated reaction schemes restricted in both the monomer scope and yield. Here, we introduce a new synthetic approach coined "μSTAR", miktoarm synthesis by termination after ring-opening metathesis polymerization, that circumvents these traditional synthetic limitations by constructing the block−block junction in a scalable one-pot process involving (1) grafting-through polymerization of a macromonomer followed by (2) in situ enyne-mediated termination to install a single mikto-arm with exceptional efficiency. This modular μSTAR platform cleanly generates AB_n and $A(BA')_n$ miktoarm star polymers with unprecedented versatility in the selection of A and B chemistries as demonstrated using many common polymer building blocks. The average number of B or BA′ arms (n) is easily controlled by the equivalents of Grubbs catalyst. While these materials are characterized by dispersity in n that arises from the statistics of polymerization, they self-assemble into mesophases that are identical to those predicted for precise miktoarm stars. In summary, the μSTAR technique provides a significant boost in design flexibility and synthetic simplicity while retaining the salient phase behavior of precise miktoarm star materials.

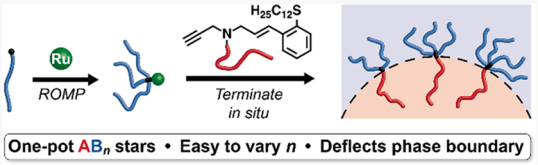

INTRODUCTION

Block copolymers (BCPs) are important in a variety of emerging and established applications due to their self-assembly into well-ordered structures on the nanometer length scale.[1] The phase behavior of linear BCPs with two chemically distinct blocks arrayed in simple sequences (AB, ABA, ...) is now well understood from both experiments[2−4] and theory[5−8] to be dependent on the Flory−Huggins interaction parameter (χ), volumetric degree of polymerization (N), block volume fractions (f_i, i = A, B), and conformational asymmetry (ε). These molecular design parameters dictate the self-assembly of two-component BCPs into a handful of classical phases[4] (body-centered cubic spheres, hexagonally close-packed cylinders, a gyroid network, and lamellae) and more exotic sphere packings[9−11] (e.g., σ, C14, C15, and A15). While the utility of many such mesophases is indisputable, linear chain connectivity imposes structure−property constraints that are not always desirable. For example, the number of known morphologies remains small,[12] domain periodicities are fairly restricted (typically within a range of ca. 5−100 nm),[13,14] and the coupling between volume fraction (f) and morphology favors the majority block on the convex side of curved block−block interfaces.[5,15] These (and other) limitations have motivated the search for new molecular design tools that broaden the utility of BCP self-assembly in contemporary applications.

An exciting opportunity that expands the confines of traditional polymer phase behavior[16] lies in the controlled synthesis of BCPs with branched architectures.[17,18] The introduction of branching imparts useful thermodynamic,[19] photonic,[20,21] and mechanical[22] properties that are otherwise inaccessible with linear analogues. One archetypal example is miktoarm star polymers,[23−32] which are defined[33] as two or more chemically distinct blocks connected to a common junction (e.g., A_mB_n, $m + n > 2$). The miktoarm star architecture is known or predicted to stabilize new phases,[9,15,34] reduce domain spacing,[35] and manipulate melt[25,26,36,37] or solution[38−40] properties, making them attractive for applications such as lithography and drug delivery. A further subset of miktoarm star polymers that accentuates the role of architecture in self-assembly involves asymmetry in arm number ($m \neq n$); here, we focus on the limit m = 1, for example, AB_n. As a result of arm asymmetry, bulk phase boundaries are significantly deflected toward larger values of the A-block volume fraction (f_A).[5,15] This effect has been beautifully exploited by Lynd et al.[41] and Shi et al.[42] to design new thermoplastic elastomers ($A(BA')_n$) that are stronger, stiffer, and tougher than commercial ABA linear triblock copolymers.

Despite the importance of miktoarm star polymers in contemporary polymer science, their synthesis still remains a major challenge. The standard approach to generate precise connectivity at a common junction uses some combination of "grafting-from" and "grafting-to" multistep reaction schemes.[43]

Received: November 11, 2019
Published: January 8, 2020

https://dx.doi.org/10.1021/acs.macromol.9b02380
Macromolecules 2020, 53, 702−710

The need for orthogonal reactivity, high yields, and designer core molecules requires tedious synthetic routes that often include time-consuming coupling, polymerization, (de)-protection, and purification steps such as fractional precipitation and high-performance liquid chromatography.[36,44,45] For example, the anionic materials studied by Shi and co-workers[42] necessitated reaction times in excess of 30 days to push coupling to high conversion and still required purification via fractionation.[45−47] Moreover, changing the number of arms is nontrivial since a new core starting material must be selected each time.

Motivated by the difficulty of traditional miktoarm star polymer syntheses, we recently exploited the versatility, speed, and efficiency of Grubbs-type ring-opening metathesis polymerization (ROMP)[48−57] to synthesize miktoarm star polymers via the grafting-through copolymerization of two different macromonomers at low backbone degrees of polymerization (N_{BB}).[58] This type of statistical copolymerization is remarkably well controlled, and the short backbone behaves physically like the core of a star polymer at $N_{BB} \lesssim 12$ as evidenced by experiments and theory. However, simple copolymerization trades molecular precision for synthetic versatility since the reaction stoichiometry can only control the average number of arms and molecular composition. As a result, bulk phase behavior is dominated by dispersity effects that counteract phase boundary deflection, even in the case of nominally asymmetric architectures. Copolymerization therefore cannot generate the unique phase behavior that distinguishes asymmetric miktoarm stars from traditional block copolymers.

Here, we introduce a new synthetic method termed μSTAR (Table 1, top), miktoarm synthesis by termination after ring-opening metathesis polymerization, that efficiently generates asymmetric miktoarm star polymers using ruthenium-catalyzed macromonomer polymerization (B → B_n) followed by in situ enyne-mediated termination[59] to install the single A arm (B_n → AB_n). μSTAR sits at an optimal synthetic intersection, combining the versatility and speed of a macromonomer approach using ROMP with the precision of a highly efficient coupling step. Using a handful of macromonomers and macroterminators as building blocks, a diverse library of miktoarm stars can be easily prepared with different numbers of arms and block chemistries. We highlight this modularity by synthesizing AB_n and $A(BA')_n$ miktoarm star polymers comprising six different permutations of A and B block chemistry selected from poly(siloxane), poly(acrylate), poly(methacrylate), poly(ether), poly(ester), and poly(styrene). The average number of B arms (n) is easily controlled by equivalents of Grubbs catalyst to the macromonomer in the initial polymerization step. Importantly, the phase behavior of these polymers with disperse n exhibits significant phase boundary deflections, in agreement with self-consistent field theory (SCFT) simulations performed on precise (monodisperse n) analogues. A major implication of this finding is that the dispersity in n produced by μSTAR is advantageous from the perspective of significantly simplifying the synthesis of miktoarm star polymers while retaining the characteristic phase behavior that produces interesting bulk properties. The speed, efficiency, and broad scope of μSTAR establishes a compelling new synthetic platform for asymmetric miktoarm star polymers and supports the notion that low dispersity is not always better in block copolymer self-assembly.[60,61]

Table 1. (Top) Generic μSTAR Synthesis of Miktoarm Star Polymers Using Norbornene-Functionalized Macromonomers and Enyne Macroterminators; (Bottom) Macromonomers, Macroterminators, and Miktoarm Star Polymers Synthesized in this Work

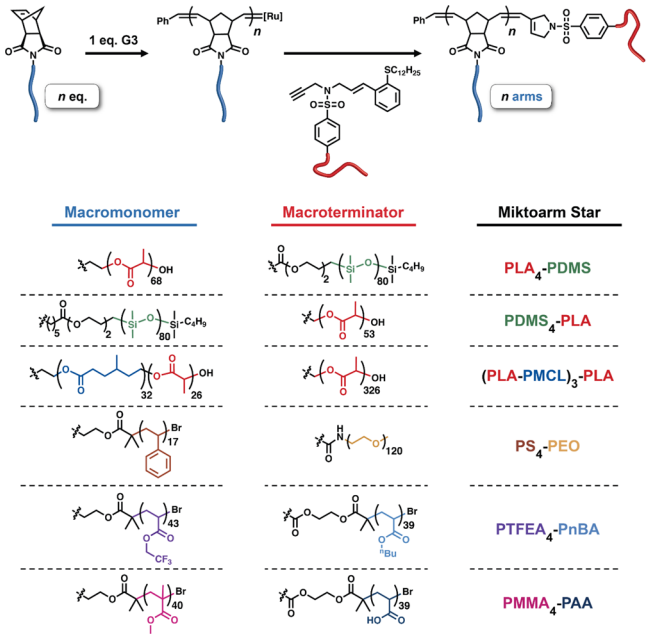

MATERIALS AND METHODS

Synthesis. Full synthetic methods are provided in the Supporting Information, including small-molecule and polymer synthesis, purification, and characterization data.

Characterization. ^{1}H and ^{13}C NMR spectra of small molecules were recorded on Bruker Avance 400 or 500 MHz instruments and calibrated using a residual undeuterated solvent as an internal reference ($CHCl_3$ at 7.26 ppm in ^{1}H NMR and 77.16 ppm in ^{13}C NMR). ^{1}H, ^{13}C, and ^{19}F NMR spectra of polymers were collected on a 600 MHz Varian VNMRS. The following abbreviations (or combinations thereof) were used to explain the multiplicities: s = singlet, d = doublet, t = triplet, q = quartet, m = multiplet, br = broad. Mass spectra (MS) were recorded on an LC/MS (Agilent Technologies 1260 Infinity II/6120 Quadrupole) instrument by ESI. Melting points were measured on a Bibby Scientific's MEL-TEMP digital melting point apparatus. Infrared (IR) spectra were recorded on a Thermo Nicolet iS10 Fourier-transform infrared (FTIR) spectrometer with a Smart Diamond attenuated total reflectance (ATR) sampling accessory. Size-exclusion chromatography with multiangle light scattering detection (SEC-MALS) was performed using two Agilent columns (PLgel, 5 μm MiniMIX-D, 250 × 4.6 mm) connected to a Waters Alliance HPLC System, 2690 separation module pump, Wyatt 18-angle DAWN HELEOS-II light scattering detector, and Wyatt REX differential refractive index detector using THF as the mobile phase. The absolute molar mass was determined by light scattering using online determination of dn/dc by assuming 100% mass elution under the peak of interest. Size-exclusion chromatography was also performed on a Waters instrument using a differential refractive index detector and two Tosoh columns (TSKgel SuperHZM-N, 3 μm polymer, 150 × 4.6 mm) with chloroform at 35 °C as the mobile phase. In this case, molar masses and molar mass dispersity ($Đ$) were determined against narrow PS standards (Agilent). ^{1}H and ^{19}F diffusion-ordered spectroscopy (DOSY) experiments were performed on a Bruker Avance III 300 MHz SWB diffusion NMR spectrometer equipped with a Diff50 z-diffusion probe using a stimulated echo sequence, bipolar gradient

https://dx.doi.org/10.1021/acs.macromol.9b02380
Macromolecules 2020, 53, 702−710

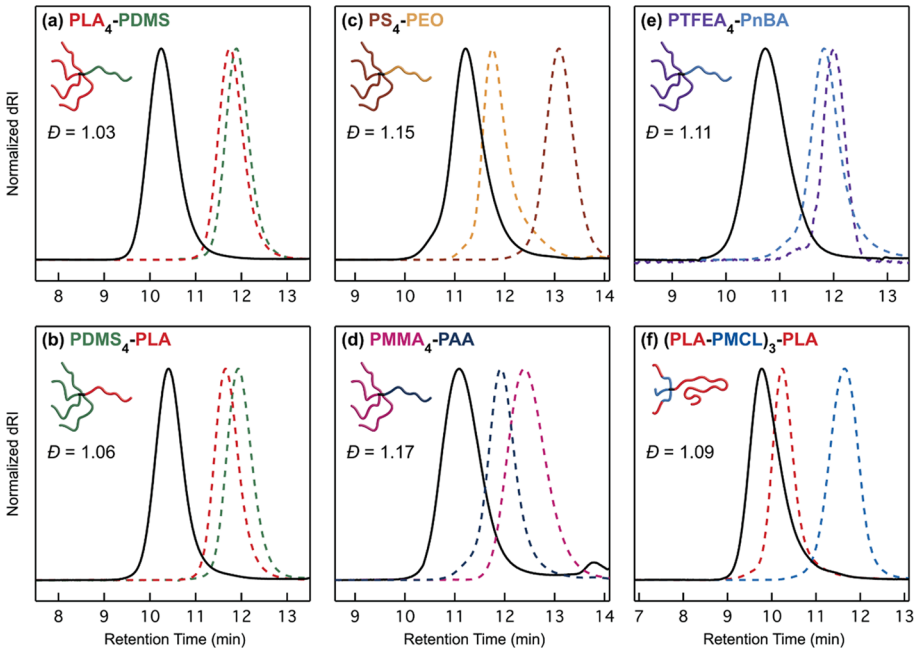

Figure 1. Size-exclusion chromatograms (normalized differential refractive index signal, dRI) of the miktoarm star polymers (solid black lines) listed in Table 1: (a) PLA_4-PDMS, (b) $PDMS_4$-PLA, (c) PS_4-PEO, (d) $PMMA_4$-PAA, (e) $PTFEA_4$-PnBA, and (f) $(PLA\text{-}PMCL)_3$-PLA. Macromonomers and macroterminators are depicted with dashed lines. See the Supporting Information (Figures S2−S10) for traces of the poly(macromonomers), which were omitted here for clarity. In (d), the macroterminator trace represents poly(*tert*-butyl acrylate) before deprotection, while the final miktoarm star curve comprises poly(acrylic acid) after deprotection. Also note that the small bump near 14 min is small-molecule elution. In (e), the PTFEA macromonomer and $PTFEA_4$-PnBA samples have negative dn/dc values in THF; the dRI data were multiplied by −1 for the purpose of consistent presentation.

(SteBp) pulse sequences,[62] 16 gradient steps, and 16 scans at each step. All DOSY experiments were run in either chloroform-d or acetone-d_6 at polymer concentrations of ∼25 mg/mL without spinning to avoid convection. DOSY data analysis was performed in Mathematica wherein the data were normalized and fit to a single exponential function. Room temperature SAXS measurements were performed at beamline 7.3.3 of the Advanced Light Source (ALS) at the Lawrence Berkeley National Laboratory in Berkeley, CA. A sample-to-detector distance of 3815 mm was used with an X-ray wavelength of 1.24 Å. Variable-temperature SAXS measurements were performed at beamline 1-5 of the Stanford Synchrotron Radiation Lightsource (SSRL) to determine order−disorder transition temperatures (T_{ODT}) using a sample-to-detector distance of 2870 mm and a 1.03 Å X-ray wavelength. Heating was performed on a custom stage with temperatures measured at the sample position to ensure accuracy. Samples were equilibrated for 5 min at each temperature before collecting scattering images. For all SAXS experiments, a silver behenate standard was used to calibrate the scattering angles. 2D data were reduced by azimuthal averaging to give $I(q)$ where I is the intensity in arbitrary units, $q = |\mathbf{q}| = 4\pi\lambda^{-1}\sin(\theta/2)$ is the magnitude of the scattering wave vector, λ is the wavelength of the incident beam, and θ is the scattering angle.

Self-Consistent Field Theory. Self-consistent field theory (SCFT) simulations were performed using the standard model of an incompressible diblock copolymer melt (model E in ref 63) using chain propagators suitably adjusted to account for the star architecture with all polymer arms extending from a single point.[63] The modified diffusion equation was solved pseudo-spectrally in the field variables using the second-order operator splitting (SOS) algorithm for the contour variable with a contour resolution of $\Delta s = 0.001$. Note that this relatively small value of Δs was necessary to sufficiently resolve the block bi-dispersity parameter τ. Field updates were performed using the semi-implicit Siedel (SIS) scheme. Phase diagrams were constructed in the standard manner by computing the free energy of different candidate phases and then determining where the free energies of two phases are equal. Candidate phases considered (and corresponding spatial resolution) were BCC spheres (32 × 32 × 32), cylinders (32 × 32), double gyroids (32 × 32 × 32), lamellae (128), and the disordered phase. The ODT was determined using the experimentally relevant f_A and adjusting χ until the free energy of the disordered and closest ordered phases were equal. The statistical segment lengths of the two blocks were assumed to be equal ($b_A/b_B = 1$). A more detailed computational study of the miktoarm architecture will be the topic of a forthcoming publication.[64]

RESULTS AND DISCUSSION

Synthesis. Two types of simple linear precursors are needed in the μSTAR process to create miktoarm polymers: a macromonomer with a single polymerizable end-group and a macroterminator that will irreversibly couple exactly once to the active chain ends. We focus on using Grubbs-type ring-opening metathesis polymerization (ROMP) to construct the junction due to its well-established functional group tolerance, fast reaction rates, and high yields.[65] Norbornene was therefore selected as the polymerizable group on the macromonomer because it undergoes efficient ROMP;[66] both homopolymer (B) and diblocks (BA′) will be discussed with norbornene installed on the B terminus. For the macroterminator, we exploit enyne-mediated termination chemistry recently developed by Gutekunst and co-workers[59] to perform macromolecular coupling of living metathesis polymers.[67,68] While enyne macroterminators were previously shown to efficiently prepare diblocks, the sterics involved in coupling to the core of a star polymer present a unique challenge.[69] Nevertheless, the high reactivity of enynes makes them suitable for macromolecular couplings that would otherwise not be possible with traditional ROMP termination methods employing substituted vinyl ethers or symmetrical *cis*-olefins.[70−74] The generic end-groups used in μSTAR are illustrated in Table 1 (top).

https://dx.doi.org/10.1021/acs.macromol.9b02380
Macromolecules 2020, 53, 702−710

Macromonomers with different B chemistries were synthesized by polymerization from functional norbornene initiators or coupling reactions between a norbornene acid and commercially available monotelechelic polymers. In summary, six different macromonomers were synthesized, which span various classes of polymer chemistry: poly(lactide) (PLA), poly(dimethylsiloxane) (PDMS), poly(4-methylcaprolactone-*block*-lactide) (PMCL-PLA), poly(styrene) (PS), poly(2-trifluoroethyl acrylate) (PTFEA), and poly(methyl methacrylate) (PMMA). Similarly, six macroterminators (A) were prepared by coupling to or directly growing from the enyne terminator molecule. PDMS, PLA, poly(ethylene oxide) (PEO), poly(*n*-butyl acrylate) (PnBA), and poly(*tert*-butyl acrylate) (PtBA) were chosen as representative A blocks (see the Supporting Information). The methyl ester enyne small molecule can be prepared in four high yielding steps and is further derivatized into the terminator of choice by one or two additional reactions.[59] Table 1 (bottom) summarizes these materials; full characterization details are provided in the Supporting Information (Schemes S1−S13, Tables S1 and S2, and Figure S1).

The efficacy of μSTAR at synthesizing asymmetric miktoarm star polymers is evident in Figure 1, which summarizes size-exclusion chromatograms (SECs) of the macromonomers (dashed lines), macroterminators (dashed lines), and resultant miktoarm star polymers (solid lines) for the combinations described in Table 1. The general process involves two steps that occur in one pot. (1) Polymerization of the macromonomer creates a short bottlebrush (N_{BB} < 12) with star-like physical properties[58] (vide infra); after complete conversion, an aliquot of the poly(macromonomer) is extracted. (2) In situ termination by the addition of macroterminators efficiently couples a single A arm to the living star polymer, resulting in AB_n or $A(BA')_n$ chain connectivity. SEC traces of the poly(macromonomers) are omitted from Figure 1 for clarity but can be found in Figures S2−S10. Note that with the exception of Figure 1f, n = 4 was targeted in this initial set of examples. Kinetic experiments performed with a model 5 kDa PLA macroterminator indicate that the coupling process is finished in approximately 2 h at room temperature (Figure S11). After termination, the increase in poly(macromonomer) absolute molecular weight as measured with multiangle light scattering (MALS) is roughly consistent with the macroterminator size (Tables S3 and S4). A single precipitation into methanol, diethyl ether, or hexanes is sufficient to isolate the final miktoarm star polymers, which have low molar mass dispersities ($Đ$ < 1.2, Table S4) and monomodal SEC traces (Figure 1). ^{1}H nuclear magnetic resonance (NMR) measurements further confirmed the stoichiometric coupling of macroterminators and poly(macromonomers) (Figures S12−S22) and were also used to calculate compositions as tabulated in Table S4. Diffusion-ordered spectroscopy (DOSY) analysis revealed that these miktoarm star polymers lack homopolymer contamination within measurement error (Tables S5 and S6 and Figures S23 and S24)[75] as attempts to determine the percentage of homopolymer contamination with multicomponent fits yielded inconsistent results and nonphysical diffusion coefficients, which is evidence of data overfitting.[76]

Another advantage of μSTAR is the ability to easily vary the average number of B or BA′ arms by changing the equivalents of macromonomer to Grubbs initiator. A series of four $A(BA')_n$ asymmetric miktoarm star polymers (A = PLA and BA′ = PMCL-*block*-PLA) with n = 3, 5, 7, or 9 arms was prepared simultaneously in separate reaction vessels using the same macromonomer and macroterminator precursors (Figure 2). SEC traces smoothly decrease in elution time as n increases, and absolute molecular weight measurements are consistent with increasing the average number of poly(macromonomer) arms across the range of n = 3−9 (Table S3). This ability to easily vary the number of arms stands in stark contrast to all previous synthetic strategies where a different initiator or core must be synthesized whenever the number of arms is varied.[29,45,77] These materials also highlight the tolerance of μSTAR chemistry to high molecular weights; for n = 9, a 54 kDa poly(macromonomer) cleanly couples to a 24 kDa PLA macroterminator using only 1.1 equiv of the latter.

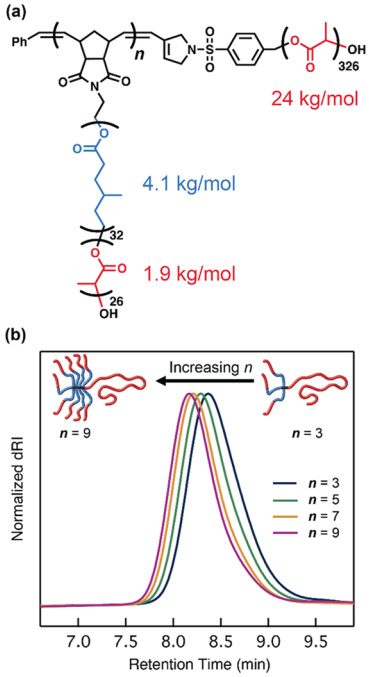

Figure 2. μSTAR can easily vary the average number of arms, n, in an asymmetric miktoarm star polymer. (a) Chemical structure of $(PLA\text{-}PMCL)_n$-PLA with n = 3−9. (b) Normalized differential refractive index signal from SEC analysis of the isolated miktoarm star polymers. See Table S4 for a summary of molecular weights and dispersities.

Self-Assembly. A key question that remains is whether asymmetric miktoarm star polymers synthesized via μSTAR (with dispersity in n) self-assemble as predicted by theory for precise analogues. We have opted to study in detail the phase behavior of the $(PLA\text{-}PMCL)_n$-PLA samples described in Figures 1 and 2 since the addition of a short A′ block flanking B is predicted to further accentuate the phase boundary deflections that are characteristic of asymmetric AB_n miktoarm star polymers.[41] The left half of Figure 3 reports synchrotron small-angle X-ray scattering (SAXS) patterns collected at room temperature after annealing $(PLA\text{-}PMCL)_n$-PLA with a varying number of PLA-PMCL diblock arms (n = 3−9) at 140 °C for 18 h. Note that the volume fraction of PLA (f_{PLA}) changes with n such that these samples span f_{PLA} = 0.58−0.71. The SAXS traces for n = 3 (f_{PLA} = 0.71), n = 5 (f_{PLA} = 0.68), and n = 7 (f_{PLA} = 0.62) can be cleanly indexed as indicated by triangles that demarcate the expected location of scattering reflections for lamellar (LAM), gyroid (GYR), and hexagonally close-packed cylinders (HEX), respectively. The n = 9 material

https://dx.doi.org/10.1021/acs.macromol.9b02380
Macromolecules 2020, 53, 702−710

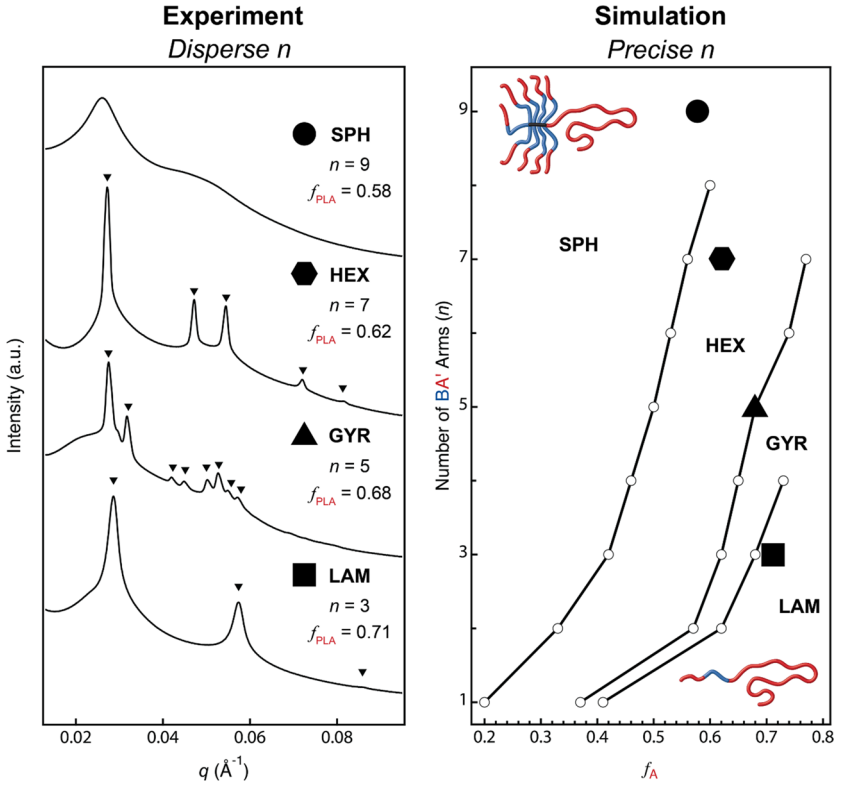

Figure 3. The phase behavior of $(PLA\text{-}PMCL)_n$-PLA miktoarm star polymers containing dispersity in n is consistent with simulations of precise analogues. Left: small-angle X-ray scattering data with triangles demarcating the expected location of Bragg reflections for lamellar (LAM, $n = 3$), gyroid (GYR, $n = 5$), and hexagonally close-packed cylinder (HEX, $n = 7$) morphologies. Right: SCFT simulations at $\tau \equiv N_A/(N_A + N_{A'}) = 0.91$ relating morphology, PLA volume fraction (f_{PLA}), and the number of PMCL-PLA (BA′) diblock arms (n) at $\chi N = 36$, which corresponds to the segregation strength at 298 K.[79] Superposed symbols represent the four experimental samples.

shows broader peaks that are less well defined, but their intensity maxima approximately coincide with those expected for a spherical form factor and Percus−Yevick structure factor[78] (Figure S25); we tentatively ascribe this morphology as disordered spheres that possibly fail to order on a well-defined lattice due to kinetic limitations. Collectively, these data are consistent with a remarkable deflection of order−order phase boundaries toward larger f_A values relative to linear AB diblock or ABA triblock copolymers. For example, the HEX−GYR transition occurs near $f_A = 0.3$ with linear diblocks versus in the vicinity of $f_A = 0.62$−0.68 that we measure for $(PLA\text{-}PMCL)_n$-PLA mikto polymers. We are confident that the PLA block resides in the interior of the cylinders since GYR ($f_{PLA} = 0.68$) and LAM ($f_{PLA} = 0.71$) occur at even larger volume fractions than HEX ($f_{PLA} = 0.62$). These experimental data relating morphology and volume fraction are in agreement with SCFT simulations performed on $A(BA')_n$ asymmetric miktoarm star polymers using the literature-reported[79] value of $\chi_{PLA\text{-}PMCL}$ and the degrees of polymerization measured experimentally for A = PLA and BA′ = PMCL-PLA (Figure 3: right; see the Supporting Information for details). We conclude that asymmetric miktoarm star polymers synthesized via μSTAR, which necessarily have dispersity in n, can self-assemble into structures that mimic precise molecular analogues.

Discussion. Historically, anionic polymerization has been the workhorse synthetic technique used to construct miktoarm star polymers, including AB_n[32,69,77,80,81] and $A(BA')_n$[42,45] asymmetric variants. While effective, rigorous purification requirements, a limited monomer scope, sequence constraints, sluggish coupling kinetics[47] (that can take months to reach full conversion), and the need for additional purification by fractional precipitation[32,45,77] are inconvenient from both practical and design perspectives. μSTAR overcomes all of these challenges, assuming that dispersity in n can be tolerated, by exploiting the well-established functional group compatibility and speed of ROMP. We note that a conceptually similar approach has been attempted with anionic polymerization in the past, namely, the grafting-through polymerization of a polystyrene (polyisoprene) macromonomer to construct the B_n core either preceded or followed by the polymerization of polyisoprene (polystyrene) to grow a single A block.[82] The result was rather broad and multimodal SEC traces, particularly for the poly(macromonomers). Despite some improvement after repeated fractional precipitation, any optimized anionic methodology would still lack the versatility of a ROMP-based approach.

The examples in Figures 1 and 2 were selected to accentuate different types of chemistry that are of contemporary importance and challenging to link together using traditional miktoarm star syntheses. For example, PLA_n-PDMS (Figure 1a) and $PDMS_n$-PLA (Figure 1b) may be useful as lithographic materials with higher resolution than linear analogues due to architecture effects while maintaining good etch contrast.[13,19,35,37,83,84] In the field of electrochemical energy storage, miktoarm star polymers containing PEO blocks are of interest as safe battery electrolytes, yet their reported synthesis is involved.[36] We have demonstrated that PS_n-PEO miktoarm stars are straightforward to synthesize with μSTAR (Figure 1c). μSTAR also provides access to amphiphilic

https://dx.doi.org/10.1021/acs.macromol.9b02380
Macromolecules 2020, 53, 702−710

miktoarm star polymers, for example, by combining a PMMA macromonomer and PtBA terminator (Figure 1d) followed by acid-catalyzed deprotection of the *tert*-butyl ester to poly(acrylic acid) (PAA). The sulfonamide−pyrroline linkage created during termination is robust enough to withstand a concentrated solution of trifluoroacetic acid and yield the partially charged $PMMA_n$-PAA star polymer (Scheme S14 and Figures S26−S29). Figure 1e further showcases a combination of acrylates ($PTFEA_4$-PnBA) that would be especially difficult to access via a core-first approach since both monomers undergo polymerization with the same type of radical initiator; the incorporation of semi-fluorinated acrylates may also create opportunities in surface coatings and other advanced materials.[85−88]

As introduced earlier, the $A(BA')_n$ architecture presents exciting opportunities for next-generation thermoplastic elastomers.[42] To date, this concept has only been explored using A, A′ = poly(styrene) (PS), and B = poly(isoprene) (PI) blocks synthesized by anionic polymerization and silyl chloride coupling.[45] Inspired by the work of Hillmyer,[79] here, we have shown that renewable types of glassy (PLA) and rubbery (PMCL) polyesters can form $A(BA')_n$ miktoarm stars with n = 3−9 using μSTAR (Figure 1f), which are inaccessible via the established anionic route. The phase behavior of $(PLA\text{-}PMCL)_n$-PLA asymmetric miktoarm star polymers synthesized with μSTAR is consistent with past experimental reports on precise $(PS\text{-}PI)_3$-PS[42] and theory that anticipate significant deflection of order−order transitions toward larger volume fractions due to molecular architecture. We have not observed this effect in any simple ROMP copolymerizations involving A and B macromonomers,[58] even at unequal feed compositions, which suggests that efficient termination chemistry (or some other method of installing a single A arm) is key to unlocking the unique self-assembly of asymmetric miktoarm star polymers. This result bolsters our previous finding that short bottlebrushes actually behave like miktoarm star polymers despite the inherent dispersity in n.[58] Note that SCFT simulations reveal a large sensitivity to the relative lengths of A and A′ blocks as parameterized by $\tau = N_A/(N_A + N_{A'})$ (Figure S30). Although our experimental calculation of τ is based on molar masses measured by NMR (τ = 0.896) and MALS (τ = 0.925) that are within reasonable experimental uncertainty, SCFT simulations match the data in Figure 3 (left) best with an intermediate of τ = 0.91 shown in Figure 3 (right). SCFT also accurately captures the temperature-dependent phase behavior of these materials. By measuring the order−disorder transition temperature (T_{ODT}) with variable-temperature SAXS (Figure S31) and calculating $\chi(T_{ODT})$ from the relationship reported by Watts,[79] $(\chi N)_{ODT}$ was compared to SCFT predictions. Incredibly, for n = 3, the theoretical and experimental values differ by less than 1% (Figure S32). As n increases, the deviation grows, but it never exceeds 12%.

We hasten to note that not all miktoarm star samples produced with μSTAR show scattering reflections that are as well-resolved as those in Figure 3. This may be the result of thermodynamic or kinetic factors that are influenced by architecture, dispersity, high molecular weight, or a combination thereof. For example, with n = 9 and f_A = 0.58 (Figure 3, left), the thermodynamically stable phase might be A15,[15,89] which is likely kinetically inaccessible above a certain threshold molecular weight.[90] Another possibility is a complex free energy landscape; Grason and co-workers have previously argued that kinetic trapping could cause a similar glassy intermediate phase in AB_2 miktoarm stars due to the near degeneracy of BCC and A15.[15] Thus, it is not surprising that complex sphere phase formation is suppressed.[10,90] Nevertheless, we find it remarkable that μSTAR can produce clean self-assembly given the dispersity in n.

Figure 4 illustrates the key differences in molecular composition and self-assembly that result from various

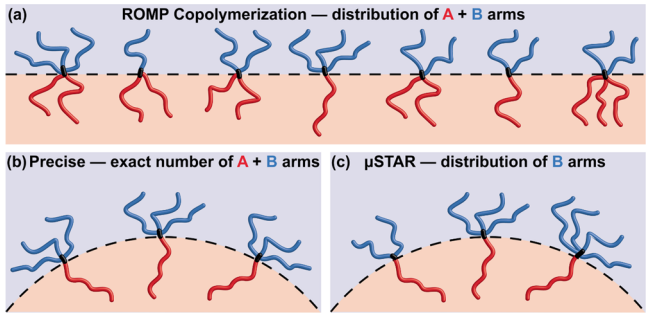

Figure 4. Illustration of molecular composition and self-assembly resulting from different miktoarm star synthesis techniques. (a) Simple ROMP copolymerization of two macromonomers generates dispersity in composition and the number of A and B arms, which promotes flat block−block interfaces.[58] (b) Asymmetric miktoarm stars (e.g., AB_3) created by precise synthesis favor interfacial curvature toward the A block.[15] (c) μSTAR produces miktoarm stars with a distribution of B arms and exactly one A arm, resulting in interfacial curvature that is similar to precise analogues with the average molecular composition.

miktoarm star synthesis techniques. Simple ROMP copolymerization with either a blocky or statistical sequence at low N_{BB} generates composition and arm-number dispersity that together tend to favor a flat block−block interface (Figure 4a).[58] At the same overall composition (i.e., f_A = 0.5), asymmetric miktoarm star polymers with a precise number of arms (for example, AB_3) bias interfacial curvature toward the A block (Figure 4b).[15,26] Samples synthesized using μSTAR sit somewhere in between. Exactly one A arm and a distribution of B arms still results in self-assembly that favors interfacial curvature, the magnitude of which is evidently similar to precise analogues with the average μSTAR composition (Figure 4c). One benefit of incorporating such dispersity lies in relaxing synthetic burden without drastically impacting self-assembly.

CONCLUSIONS

In summary, we have introduced a new synthetic technique termed μSTAR that generates AB_n and $A(BA')_n$ asymmetric miktoarm star polymers using grafting-through polymerization and efficient enyne-mediated polymer−polymer coupling chemistry. This modular approach is compatible with a wide variety of polymer chemistries and can accommodate high molecular weight arms. The average number of B or BA′ arms (n) is easily varied by the ratio of Grubbs catalyst to the macromonomer in the initial polymerization step. Miktoarm star polymers made via μSTAR exhibit large deflections in the block copolymer phase diagram (relative to linear analogues) unlike stars produced by statistical grafting-through copolymerization. Despite the dispersity in n, experimental phase behavior matches SCFT calculations performed with precise molecular connectivity. μSTAR significantly simplifies the

https://dx.doi.org/10.1021/acs.macromol.9b02380
Macromolecules 2020, 53, 702−710

synthesis of asymmetric miktoarm star polymers when dispersity in arm number can be tolerated.

■ ASSOCIATED CONTENT

Supporting Information

The Supporting Information is available free of charge at https://pubs.acs.org/doi/10.1021/acs.macromol.9b02380.

Full synthetic procedures and characterization, NMR DOSY analysis, SAXS fitting, and comparison of experiments with SCFT simulations (PDF)

■ AUTHOR INFORMATION

Corresponding Author

Christopher M. Bates − *University of California, Santa Barbara, California;* orcid.org/0000-0002-1598-794X; Email: cbates@ucsb.edu

Other Authors

Adam E. Levi − *University of California, Santa Barbara, California*

Liangbing Fu − *Georgia Institute of Technology, Atlanta, Georgia*

Joshua Lequieu − *University of California, Santa Barbara, California;* orcid.org/0000-0001-9480-0989

Jacob D. Horne − *University of California, Santa Barbara, California*

Jacob Blankenship − *University of California, Santa Barbara, California*

Sanjoy Mukherjee − *University of California, Santa Barbara, California;* orcid.org/0000-0001-6810-9502

Tianqi Zhang − *Georgia Institute of Technology, Atlanta, Georgia*

Glenn H. Fredrickson − *University of California, Santa Barbara, California;* orcid.org/0000-0002-6716-9017

Will R. Gutekunst − *Georgia Institute of Technology, Atlanta, Georgia;* orcid.org/0000-0002-2427-4431

Complete contact information is available at: https://pubs.acs.org/10.1021/acs.macromol.9b02380

Author Contributions

The manuscript was written by A.E.L., L.F., W.R.G., and C.M.B. Experiments were designed by A.E.L., L.F., W.R.G., and C.M.B. and performed by A.E.L., L.F., J.D.H., J.B., S.M., and T.Z. Simulations were designed by J.L. and G.H.F. and performed by J.L. All authors have given approval to the final version of the manuscript.

Notes

The authors declare no competing financial interest.

■ ACKNOWLEDGMENTS

This material is based upon work supported by the U.S. Department of Energy, Office of Basic Energy Sciences, under award no. DE-SC0019001. A.E.L. and J.B. thank the Mellichamp Academic Initiative in Sustainability for summer fellowships. W.R.G. acknowledges the Georgia Institute of Technology for start-up funds and the National Institutes of Health under award no. R35GM133784. The research reported here made use of shared facilities of the UCSB NSF MRSEC (DMR-1720256), a member of the Materials Research Facilities Network (www.mrfn.org). X-ray scattering experiments were performed at the Advanced Light Source (a U.S. Department of Energy (DOE) Office of Science User Facility, DE-AC02-05CH11231; beamline 7.3.3) and the Stanford Synchrotron Radiation Lightsource (supported by the U.S. DOE Office of Science, Office of Basic Energy Sciences, DEAC02-76SF00515; beamline 1-5). We also acknowledge support from the Center for Scientific Computing from the CNSI, MRL: an NSF MRSEC (DMR-1720256) and NSF CNS-1725797. The authors thank Craig J. Hawker and his group for the helpful discussion and Dr. Rachel Behrens (UCSB) and Dr. Cheng Zhang for assistance in polymer characterization and analysis.

■ REFERENCES

(1) Bates, F. S.; Hillmyer, M. A.; Lodge, T. P.; Bates, C. M.; Delaney, K. T.; Fredrickson, G. H. Multiblock Polymers: Panacea or Pandora's Box? *Science* **2012**, *336*, 434−440.

(2) Hajduk, D. A.; Harper, P. E.; Gruner, S. M.; Honeker, C. C.; Kim, G.; Thomas, E. L.; Fetters, L. J. The Gyroid: A New Equilibrium Morphology in Weakly Segregated Diblock Copolymers. *Macromolecules* **1994**, *27*, 4063−4075.

(3) Bates, F. S.; Schulz, M. F.; Khandpur, A. K.; Förster, S.; Rosedale, J. H.; Almdal, K.; Mortensen, K. Fluctuations, Conformational Asymmetry and Block Copolymer Phase Behaviour. *Faraday Discuss.* **1994**, *98*, 7−18.

(4) Bates, F. S.; Fredrickson, G. H. Block Copolymer Thermodynamics: Theory And Experiment. *Annu. Rev. Phys. Chem.* **1990**, *41*, 525−557.

(5) Milner, S. T. Chain Architecture and Asymmetry in Copolymer Microphases. *Macromolecules* **1994**, *27*, 2333−2335.

(6) Leibler, L. Theory of Microphase Separation in Block Copolymers. *Macromolecules* **1980**, *13*, 1602−1617.

(7) Matsen, M. W.; Schick, M. Stable and Unstable Phases of a Diblock Copolymer Melt. *Phys. Rev. Lett.* **1994**, *72*, 2660−2663.

(8) Matsen, M. W.; Bates, F. S. Unifying Weak- and Strong-Segregation Block Copolymer Theories. *Macromolecules* **1996**, *29*, 1091−1098.

(9) Li, W.; Duan, C.; Shi, A. C. Nonclassical Spherical Packing Phases Self-Assembled from AB-Type Block Copolymers. *ACS Macro Lett.* **2017**, *6*, 1257−1262.

(10) Bates, M. W.; Lequieu, J.; Barbon, S. M.; Lewis, R. M., III; Delaney, K. T.; Anastasaki, A.; Hawker, C. J.; Fredrickson, G. H.; Bates, C. M. Stability of the A15 Phase in Diblock Copolymer Melts. *Proc. Natl. Acad. Sci. U. S. A.* **2019**, *116*, 13194−13199.

(11) Kim, K.; Schulze, M. W.; Arora, A.; Lewis, R. M., III; Hillmyer, M. A.; Dorfman, K. D.; Bates, F. S. Thermal Processing of Diblock Copolymer Melts Mimics Metallurgy. *Science* **2017**, *356*, 520−523.

(12) Bates, C. M.; Bates, F. S. 50th Anniversary Perspective: Block Polymers-Pure Potential. *Macromolecules* **2017**, *50*, 3−22.

(13) Sinturel, C.; Bates, F. S.; Hillmyer, M. A. High χ-Low N Block Polymers: How Far Can We Go? *ACS Macro Lett.* **2015**, *4*, 1044−1050.

(14) Jeong, S.-J.; Kim, J. Y.; Kim, B. H.; Moon, H. S.; Kim, S.-O. Directed Self-Assembly of Block Copolymers for next Generation Nanolithography. *Mater. Today* **2013**, *16*, 468−476.

(15) Grason, G. M.; Kamien, R. D. Interfaces in Diblocks: A Study of Miktoarm Star Copolymers. *Macromolecules* **2004**, *37*, 7371−7380.

(16) Bates, F. S. Polymer-Polymer Phase Behavior. *Science* **1991**, *251*, 898.

(17) Le, A. N.; Liang, R.; Zhong, M. Synthesis and Self-Assembly of Mixed-Graft Block Copolymers. *Chem. - Eur. J.* **2019**, *25*, 8177−8189.

(18) Polymeropoulos, G.; Zapsas, G.; Ntetsikas, K.; Bilalis, P.; Gnanou, Y.; Hadjichristidis, N. 50th Anniversary Perspective:

Polymers with Complex Architectures. *Macromolecules* **2017**, *50*, 1253−1290.
(19) Guo, Z.-H.; Le, A. N.; Feng, X.; Choo, Y.; Liu, B.; Wang, D.; Wan, Z.; Gu, Y.; Zhao, J.; Li, V.; Osuji, C. O.; Johnson, J. A.; Zhong, M. Janus Graft Block Copolymers: Design of a Polymer Architecture for Independently Tuned Nanostructures and Polymer Properties. *Angew. Chem, Int. Ed.* **2018**, *57*, 8493−8497.
(20) Sveinbjörnsson, B. R.; Weitekamp, R. A.; Miyake, G. M.; Xia, Y.; Atwater, H. A.; Grubbs, R. H. Rapid Self-Assembly of Brush Block Copolymers to Photonic Crystals. *Proc. Natl. Acad. Sci. U. S. A.* **2012**, *109*, 14332−14336.
(21) Vatankhah-Varnosfaderani, M.; Keith, A. N.; Cong, Y.; Liang, H.; Rosenthal, M.; Sztucki, M.; Clair, C.; Magonov, S.; Ivanov, D. A.; Dobrynin, A. V.; Sheiko, S. S. Chameleon-like Elastomers with Molecularly Encoded Strain-Adaptive Stiffening and Coloration. *Science* **2018**, *359*, 1509−1513.
(22) Wang, H.; Lu, W.; Wang, W.; Shah, P. N.; Misichronis, K.; Kang, N.-G.; Mays, J. W. Design and Synthesis of Multigraft Copolymer Thermoplastic Elastomers: Superelastomers. *Macromol. Chem. Phys.* **2018**, *219*, 1700254.
(23) Li, Z.; Kesselman, E.; Talmon, Y.; Hillmyer, M. A.; Lodge, T. P. Multicompartment Micelles from ABC Miktoarm Stars in Water. *Science* **2004**, *306*, 98−101.
(24) *Miktoarm Star Polymers: From Basics of Branched Architecture to Synthesis, Self-Assembly and Applications*; Kakkar, A., Ed.; The Royal Society of Chemistry, 2017.
(25) Yang, L.; Hong, S.; Gido, S. P.; Velis, G.; Hadjichristidis, N. I5S Miktoarm Star Block Copolymers: Packing Constraints on Morphology and Discontinuous Chevron Tilt Grain Boundaries. *Macromolecules* **2001**, *34*, 9069−9073.
(26) Beyer, F. L.; Gido, S. P.; Velis, G.; Hadjichristidis, N.; Tan, N. B. Morphological Behavior of A5B Miktoarm Star Block Copolymers. *Macromolecules* **1999**, *32*, 6604−6607.
(27) Pochan, D. J.; Gido, S. P.; Pispas, S.; Mays, J. W. Morphological Transitions in an I2S Simple Graft Block Copolymer: From Folded Sheets to Folded Lace to Randomly Oriented Worms at Equilibrium. *Macromolecules* **1996**, *29*, 5099−5105.
(28) Pochan, D. J.; Gido, S. P.; Zhou, J.; Mays, J. W.; Whitmore, M.; Ryan, A. J. Morphologies of Microphase-separated Conformationally Asymmetric Diblock Copolymers. *J. Polym. Sci., Part B: Polym. Phys.* **1997**, *35*, 2629−2643.
(29) Beyer, F. L.; Gido, S. P.; Poulos, Y.; Avgeropoulos, A.; Hadjichristidis, N. Morphology of Vergina Star 16-Arm Block Copolymers and Scaling Behavior of Interfacial Area with Graft Point Functionality. *Macromolecules* **1997**, *30*, 2373−2376.
(30) Gido, S. P.; Lee, C.; Pochan, D. J.; Pispas, S.; Mays, J. W.; Hadjichristidis, N. Synthesis, Characterization, and Morphology of Model Graft Copolymers with Trifunctional Branch Points. *Macromolecules* **1996**, *29*, 7022−7028.
(31) Hadjichristidis, N.; Iatrou, H.; Behal, S. K.; Chludzinski, J. J.; Disko, M. M.; Garner, R. T.; Liang, K. S.; Lohse, D. J.; Milner, S. T. Morphology and Miscibility of Miktoarm Styrene-Diene Copolymers and Terpolymers. *Macromolecules* **1993**, *26*, 5812−5815.
(32) Tselikas, Y.; Iatrou, H.; Hadjichristidis, N.; Liang, K. S.; Mohanty, K.; Lohse, D. J. Morphology of Miktoarm Star Block Copolymers of Styrene and Isoprene. *J. Chem. Phys.* **1996**, *105*, 2456−2462.
(33) Iatrou, H.; Hadjichristidis, N. Synthesis and Characterization of Model 4-Miktoarm Star Co- and Quaterpolymers. *Macromolecules* **1993**, *26*, 2479−2484.
(34) Aissou, K.; Choi, H. K.; Nunns, A.; Manners, I.; Ross, C. A. Ordered Nanoscale Archimedean Tilings of a Templated 3-Miktoarm Star Terpolymer. *Nano Lett.* **2013**, *13*, 835−839.
(35) Shi, W.; Tateishi, Y.; Li, W.; Hawker, C. J.; Fredrickson, G. H.; Kramer, E. J. Producing Small Domain Features Using Miktoarm Block Copolymers with Large Interaction Parameters. *ACS Macro Lett.* **2015**, *4*, 1287−1292.
(36) Lee, D.; Jung, H. Y.; Park, M. J. Solid-State Polymer Electrolytes Based on AB_3-Type Miktoarm Star Copolymers. *ACS Macro Lett.* **2018**, *7*, 1046−1050.
(37) Minehara, H.; Pitet, L. M.; Kim, S.; Zha, R. H.; Meijer, E. W.; Hawker, C. J. Branched Block Copolymers for Tuning of Morphology and Feature Size in Thin Film Nanolithography. *Macromolecules* **2016**, *49*, 2318−2326.
(38) Kakkar, A.; Traverso, G.; Farokhzad, O. C.; Weissleder, R.; Langer, R. Evolution of Macromolecular Complexity in Drug Delivery Systems. *Nat. Rev. Chem.* **2017**, *1*, No. 0063.
(39) Lin, W.; Nie, S.; Zhong, Q.; Yang, Y.; Cai, C.; Wang, J.; Zhang, L. Amphiphilic Miktoarm Star Copolymer $(PCL)_3$-(PDEAEMA-b-PPEGMA)$_3$ as PH-Sensitive Micelles in the Delivery of Anticancer Drug. *J. Mater. Chem. B* **2014**, *2*, 4008−4020.
(40) Gelissen, A. P. H.; Pergushov, D. V.; Plamper, F. A. Janus-like Interpolyelectrolyte Complexes Based on Miktoarm Stars. *Polymer* **2013**, *54*, 6877−6881.
(41) Lynd, N. A.; Oyerokun, F. T.; O'Donoghue, D. L.; Handlin, D. L., Jr.; Fredrickson, G. H. Design of Soft and Strong Thermoplastic Elastomers Based on Nonlinear Block Copolymer Architectures Using Self-Consistent-Field Theory. *Macromolecules* **2010**, *43*, 3479−3486.
(42) Shi, W.; Lynd, N. A.; Montarnal, D.; Luo, Y.; Fredrickson, G. H.; Kramer, E. J.; Ntaras, C.; Avgeropoulos, A.; Hexemer, A. Toward Strong Thermoplastic Elastomers with Asymmetric Miktoarm Block Copolymer Architectures. *Macromolecules* **2014**, *47*, 2037−2043.
(43) Ren, J. M.; McKenzie, T. G.; Fu, Q.; Wong, E. H. H.; Xu, J.; An, Z.; Shanmugam, S.; Davis, T. P.; Boyer, C.; Qiao, G. G. Star Polymers. *Chem. Rev.* **2016**, *116*, 6743−6836.
(44) Liu, H.; Pan, W.; Tong, M.; Zhao, Y. Synthesis and Properties of Couplable ABCDE Star Copolymers by Orthogonal CuAAC and Diels-Alder Click Reactions. *Polym. Chem.* **2016**, *7*, 1603−1611.
(45) Avgeropoulos, A.; Hadjichristidis, N. Synthesis of Model Nonlinear Block Copolymers of $A(BA)_2$, $A(BA)_3$, and $(AB)_3A(BA)_3$ Type. *J. Polym. Sci., Part A: Polym. Chem.* **1997**, *35*, 813−816.
(46) Avgeropoulos, A.; Dair, B. J.; Hadjichristidis, N.; Thomas, E. L. Tricontinuous Double Gyroid Cubic Phase in Triblock Copolymers of the ABA Type. *Macromolecules* **1997**, *30*, 5634−5642.
(47) Zhu, Y.; Gido, S. P.; Moshakou, M.; Iatrou, H.; Hadjichristidis, N.; Park, S.; Chang, T. Effect of Junction Point Functionality on the Lamellar Spacing of Symmetric (PS)n(PI)n Miktoarm Star Block Copolymers. *Macromolecules* **2003**, *36*, 5719−5724.
(48) Shibuya, Y.; Nguyen, H. V.-T.; Johnson, J. A. Mikto-Brush-Arm Star Polymers via Cross-Linking of Dissimilar Bottlebrushes: Synthesis and Solution Morphologies. *ACS Macro Lett.* **2017**, *6*, 963−968.
(49) Burts, A. O.; Gao, A. X.; Johnson, J. A. Brush-First Synthesis of Core-Photodegradable Miktoarm Star Polymers via ROMP: Towards Photoresponsive Self-Assemblies. *Macromol. Rapid Commun.* **2014**, *35*, 168−173.
(50) Gorodetskaya, I. A.; Choi, T.-L.; Grubbs, R. H. Hyperbranched Macromolecules via Olefin Metathesis. *J. Am. Chem. Soc.* **2007**, *129*, 12672−12673.
(51) Liu, J.; Burts, A. O.; Li, Y.; Zhukhovitskiy, A. V.; Ottaviani, M. F.; Turro, N. J.; Johnson, J. A. "Brush-First" Method for the Parallel Synthesis of Photocleavable, Nitroxide-Labeled Poly(Ethylene Glycol) Star Polymers. *J. Am. Chem. Soc.* **2012**, *134*, 16337−16344.
(52) Dutertre, F.; Bang, K.-T.; Vereroudakis, E.; Loppinet, B.; Yang, S.; Kang, S.-Y.; Fytas, G.; Choi, T.-L. Conformation of Tunable Nanocylinders: Up to Sixth-Generation Dendronized Polymers via Graft-Through Approach by ROMP. *Macromolecules* **2019**, *52*, 3342−3350.
(53) Xia, Y.; Olsen, B. D.; Kornfield, J. A.; Grubbs, R. H. Efficient Synthesis of Narrowly Dispersed Brush Copolymers and Study of Their Assemblies: The Importance of Side Chain Arrangement. *J. Am. Chem. Soc.* **2009**, *131*, 18525−18532.
(54) Xia, Y.; Kornfield, J. A.; Grubbs, R. H. Efficient Synthesis of Narrowly Dispersed Brush Polymers via Living Ring-Opening Metathesis Polymerization of Macromonomers. *Macromolecules* **2009**, *42*, 3761−3766.

https://dx.doi.org/10.1021/acs.macromol.9b02380
Macromolecules 2020, 53, 702−710

(55) Teo, Y. C.; Xia, Y. Facile Synthesis of Macromonomers via ATRP-Nitroxide Radical Coupling and Well-Controlled Brush Block Copolymers. *Macromolecules* **2019**, *52*, 81−87.
(56) Walsh, D. J.; Guironnet, D. Macromolecules with Programmable Shape, Size, and Chemistry. *Proc. Natl. Acad. Sci. U. S. A.* **2019**, *116*, 1538−1542.
(57) Kawamoto, K.; Zhong, M.; Gadelrab, K. R.; Cheng, L.-C.; Ross, C. A.; Alexander-Katz, A.; Johnson, J. A. Graft-through Synthesis and Assembly of Janus Bottlebrush Polymers from A-Branch-B Diblock Macromonomers. *J. Am. Chem. Soc.* **2016**, *138*, 11501−11504.
(58) Levi, A. E.; Lequieu, J.; Horne, J. D.; Bates, M. W.; Ren, J. M.; Delaney, K. T.; Fredrickson, G. H.; Bates, C. M. Miktoarm Stars via Grafting-Through Copolymerization: Self-Assembly and the Star-to-Bottlebrush Transition. *Macromolecules* **2019**, *52*, 1794−1802.
(59) Fu, L.; Zhang, T.; Fu, G.; Gutekunst, W. R. Relay Conjugation of Living Metathesis Polymers. *J. Am. Chem. Soc.* **2018**, *140*, 12181−12188.
(60) Lutz, J.-F.; Ouchi, M.; Liu, D. R.; Sawamoto, M. Sequence-Controlled Polymers. *Science* **2013**, *341*, 1238149.
(61) Widin, J. M.; Schmitt, A. K.; Schmitt, A. L.; Im, K.; Mahanthappa, M. K. Unexpected Consequences of Block Polydispersity on the Self-Assembly of ABA Triblock Copolymers. *J. Am. Chem. Soc.* **2012**, *134*, 3834−3844.
(62) Wu, D.; Chen, A.; Johnson, C. S., Jr. An Improved Diffusion-Ordered Spectroscopy Experiment Incorporating Bipolar-Gradient Pulses. *J. Magn. Reson., Ser. A* **1995**, *115*, 260−264.
(63) Fredrickson, G. *The Equilibrium Theory of Inhomogeneous Polymers*; Oxford University Press: Oxford, New York, 2005, DOI: 10.1093/acprof:oso/9780198567295.001.0001.
(64) Lequieu, J.; Trenton, K.; Delaney, K. T.; Fredrickson, G. H. Extreme Deflection of Phase Boundaries with A(BA')n Miktoarm Star Polymers. *Macromolecules*, in press, DOI: 10.1021/acs.macromol.9b02254.
(65) Ogba, O. M.; Warner, N. C.; O'Leary, D. J.; Grubbs, R. H. Recent Advances in Ruthenium-Based Olefin Metathesis. *Chem. Soc. Rev.* **2018**, *47*, 4510−4544.
(66) Jha, S.; Dutta, S.; Bowden, N. B. Synthesis of Ultralarge Molecular Weight Bottlebrush Polymers Using Grubbs' Catalysts. *Macromolecules* **2004**, *37*, 4365−4374.
(67) Elling, B. R.; Xia, Y. Efficient and Facile End Group Control of Living Ring-Opening Metathesis Polymers via Single Addition of Functional Cyclopropenes. *ACS Macro Lett.* **2018**, *7*, 656−661.
(68) Elling, B. R.; Su, J. K.; Feist, J. D.; Xia, Y. Precise Placement of Single Monomer Units in Living Ring-Opening Metathesis Polymerization. *Chem* **2019**, 2691−2701.
(69) Mavroudis, A.; Avgeropoulos, A.; Hadjichristidis, N.; Thomas, E. L.; Lohse, D. J. Synthesis and Morphological Behavior of Model Linear and Miktoarm Star Copolymers of 2-Methyl-1,3-Pentadiene and Styrene. *Chem. Mater.* **2003**, *15*, 1976−1983.
(70) Matson, J. B.; Grubbs, R. H. Monotelechelic Poly(Oxa)-Norbornenes by Ring-Opening Metathesis Polymerization Using Direct End-Capping and Cross-Metathesis. *Macromolecules* **2010**, *43*, 213−221.
(71) Hilf, S.; Kilbinger, A. F. M. Thiol-Functionalized ROMP Polymers via Sacrificial Synthesis. *Macromolecules* **2009**, *42*, 4127−4133.
(72) Hilf, S.; Grubbs, R. H.; Kilbinger, A. F. M. End Capping Ring-Opening Olefin Metathesis Polymerization Polymers with Vinyl Lactones. *J. Am. Chem. Soc.* **2008**, *130*, 11040−11048.
(73) Gordon, E. J.; Gestwicki, J. E.; Strong, L. E.; Kiessling, L. L. Synthesis of End-Labeled Multivalent Ligands for Exploring Cell-Surface-Receptor-Ligand Interactions. *Chem. Biol.* **2000**, *7*, 9−16.
(74) Hilf, S.; Kilbinger, A. F. M. Functional End Groups for Polymers Prepared Using Ring-Opening Metathesis Polymerization. *Nat. Chem.* **2009**, *1*, 537−546.
(75) Yu, Q.; Pichugin, D.; Cruz, M.; Guerin, G.; Manners, I.; Winnik, M. A. NMR Study of the Dissolution of Core-Crystalline Micelles. *Macromolecules* **2018**, *51*, 3279−3289.
(76) Gauch, H. G., Jr. Prediction, Parsimony and Noise. *Am. Sci.* **1993**, *81*, 468−478.
(77) Velis, G.; Hadjichristidis, N. Synthesis of Model $PS(PI)_5$ and $(PI)_5PS(PI)_5$ Nonlinear Block Copolymers of Styrene (S) and Isoprene (I). *Macromolecules* **1999**, *32*, 534−536.
(78) Bates, C. M.; Chang, A. B.; Schulze, M. W.; Momčilović, N.; Jones, S. C.; Grubbs, R. H. Brush Polymer Ion Gels. *J. Polym. Sci., Part B: Polym. Phys.* **2016**, *54*, 292−300.
(79) Watts, A.; Kurokawa, N.; Hillmyer, M. A. Strong, Resilient, and Sustainable Aliphatic Polyester Thermoplastic Elastomers. *Biomacromolecules* **2017**, *18*, 1845−1854.
(80) Lee, C.; Gido, S. P.; Pitsikalis, M.; Mays, J. W.; Tan, N. B.; Trevino, S. F.; Hadjichristidis, N. Asymmetric Single Graft Block Copolymers: Effect of Molecular Architecture on Morphology. *Macromolecules* **1997**, *30*, 3732−3738.
(81) Iatrou, H.; Siakali-Kioulafa, E.; Hadjichristidis, N.; Roovers, J.; Mays, J. Hydrodynamic Properties of Model 3-miktoarm Star Copolymers. *J. Polym. Sci., Part B: Polym. Phys.* **1995**, *33*, 1925−1932.
(82) Se, K.; Hayashino, Y. Anionic Living Polymerization of Macromonomers : Preparation of (A)n-Star-(B)1 Star Block Copolymers and Some Properties of the Products Obtained. *Macromolecules* **2007**, *40*, 429−437.
(83) Rodwogin, M. D.; Spanjers, C. S.; Leighton, C.; Hillmyer, M. A. Polylactide-Poly(Dimethylsiloxane)- Polylactide Triblock Copolymers as Multifunctional Materials for Nanolithographic Applications. *ACS Nano* **2010**, *4*, 725−732.
(84) Pitet, L. M.; Wuister, S. F.; Peeters, E.; Kramer, E. J.; Hawker, C. J.; Meijer, E. W. Well-Organized Dense Arrays of Nanodomains in Thin Films of Poly(Dimethylsiloxane)-b-Poly(Lactide) Diblock Copolymers. *Macromolecules* **2013**, *46*, 8289−8295.
(85) Kassis, C. M.; Steehler, J. K.; Betts, D. E.; Guan, Z.; Romack, T. J.; DeSimone, J. M.; Linton, R. W. XPS Studies of Fluorinated Acrylate Polymers and Block Copolymers with Polystyrene. *Macromolecules* **1996**, *29*, 3247−3254.
(86) Zhang, J.; Clark, M. B.; Wu, C.; Li, M.; Trefonas, P., III; Hustad, P. D. Orientation Control in Thin Films of a High-χ Block Copolymer with a Surface Active Embedded Neutral Layer. *Nano Lett.* **2016**, *16*, 728−735.
(87) Morita, M.; Ogisu, H.; Kubo, M. Surface Properties of Perfluoroalkylethyl Acrylate/n-Alkyl acrylate copolymers. *J. Appl. Polym. Sci.* **1999**, 1741−1749.
(88) Fu, C.; Zhang, C.; Peng, H.; Han, F.; Baker, C.; Wu, Y.; Ta, H.; Whittaker, A. K. Enhanced Performance of Polymeric ^{19}F MRI Contrast Agents through Incorporation of Highly Water-Soluble Monomer MSEA. *Macromolecules* **2018**, *51*, 5875−5882.
(89) Xie, N.; Li, W.; Qiu, F.; Shi, A.-C. σ Phase Formed in Conformationally Asymmetric AB-Type Block Copolymers. *ACS Macro Lett.* **2014**, *3*, 906−910.
(90) Lewis, R. M., III; Arora, A.; Beech, H. K.; Lee, B.; Lindsay, A. P.; Lodge, T. P.; Dorfman, K. D.; Bates, F. S. Role of Chain Length in the Formation of Frank-Kasper Phases in Diblock Copolymers. *Phys. Rev. Lett.* **2018**, *121*, 208002.